Delivery of loaded MR1 Monomer Results in Efficient Ligand Exchange to Host MR1 and Subsequent MR1T cell activation

[Corinna A. Kulicke[1], Gwendolyn M. Swarbrick[2]], Nicole A. Ladd[3], Meghan Cansler[2], Megan Null[2], Aneta Worley[1], Chance Lemon[1], Tania Ahmed[2], Joshua Bennett[2], Deborah A. Lewinsohn[2], Erin J. Adams[3], David M. Lewinsohn[1,4], Melanie J. Harriff*[1,4]

Affiliations

[1]Division of Pulmonary, Allergy, and Critical Care Medicine, Oregon Health & Science University, Portland, OR 97239, USA

[2]Division of Infectious Diseases, Department of Pediatrics, Oregon Health & Science University, Portland, OR 97239, USA

[3]Department of Biochemistry and Molecular Biology, University of Chicago, Chicago, IL 60637, USA

[4]VA Portland Health Care System, Portland, OR 97239, USA

* corresponding author: harriffm@ohsu.edu

Keywords

MAIT cells, MAIT cell ligands, MR1-restricted T cells, antigen presentation, cellular immune response, mucosal immunology, T-cell

Abstract

MR1 restricted T (MR1T) cells have the potential to be important players in microbial infections, sterile inflammation, wound healing and cancer. Similar to other antigen presentation molecules, evidence supports multiple, complementary MR1 antigen presentation pathways. To investigate post-ER pathways for MR1 loading, we used MR1 monomers and tetramers loaded with 5-(2-oxopropylideneamino)-6-d-ribitylaminouracil (5-OP-RU) to deliver the antigen. Using MR1-deficient cells reconstituted with wild-type MR1 or MR1 molecules that cannot bind 5-OP-RU, we

show that presentation of monomer-delivered 5-OPRU is dependent on host MR1 and requires the transfer of ligand from the soluble molecule onto MR1 expressed by the antigen presenting cell in post-ER compartments. We propose a model where chaperones direct the exchange of covalently bound ligands from one MR1 molecule to another. This new mode of ligand delivery strengthens the evidence for a post-ER exchange pathway for MR1, which could represent an important avenue by which MR1 acquires antigens derived from endocytosed pathogens.

Introduction

MR1-restricted T (MR1T) cells are increasingly being recognized for their role in early responses to microbial infection, but also in non-infectious conditions including a variety of autoimmune disorders, wound healing and cancer (reviewed e.g. in [1-5]). Despite the heightened interest in these non-classical donor-unrestricted T cells, the mechanisms governing the presentation of MR1T cell antigens remain incompletely defined.

In essence, antigen presentation requires three steps: the antigen presenting molecule must leave the ER, it must bind an antigen, and it must display the bound antigen at the cell surface for T cell receptor (TCR) recognition. These basic features are shared by all antigen presentation pathways but how they are achieved mechanistically, what compartments they take place in, and in what sequence they occur differs substantially. For classical major histocompatibility complex (MHC) I/peptide complexes, antigen binding generally precedes, and is indeed required for, ER egress and is followed by translocation to the cell surface (reviewed e.g. in [6]). MHC II and CD1 molecules, by contrast, exit the ER bound to a surrogate ligand which is exchanged for antigenic ligand in the endosomal compartment after internalization from the cell surface (reviewed e.g. in [7, 8]).

For the non-classical MHC class I-related molecule 1 (MR1), evidence points towards an MHC I-like mode of antigen acquisition in that more MR1 associates with its smaller subunit β_2-microglobulin (b2m) and acquires endoglycosidase H (EndoH) resistance upon addition of ligand to the culture medium [9, 10]. In line with this, McWilliam, Mak, et al. have used a fluorescently

labelled MR1 antigen analogue to directly demonstrate loading of exogenous ligand in the ER [10]. Some studies have linked the mechanism for MR1 ER egress to the neutralization of a charged amino acid in the MR1 ligand binding groove – presumably resulting in a conformational change conducive to ER egress [9, 10]. The most potent MR1 ligand described to date, 5-(2-oxopropylideneamino)-6-D-ribitylaminouracil (5-OP-RU), forms a Schiff base with this Lysine residue, resulting in its neutralization [9, 11].

However, recent findings support the hypothesis that there are complementary, non-exclusive presentation pathways for MR1, allowing the molecule to survey diverse intracellular environments [12-19]. In particular, multiple lines of evidence suggest that ligand exchange can occur on pre-loaded MR1 molecules and that this may take place in an endosomal compartment. Most notably, releasing MR1 from the ER prior to antigen exposure by pre-incubation with the MR1 ligand 6-formylpterin (6-FP) enhances presentation of exogenous antigenic ligand to MR1T cells [13]. In line with this, siRNA knock-down of proteins involved in the trafficking and recycling of endosomal vesicles such as VAMP4, Rab6 [12], Stx4, Stx16, and VAMP2 [13] impairs MR1-mediated antigen presentation. Based on these observations, we and others have proposed ligand exchange in a post-ER compartment as a complementary mechanism for MR1 ligand acquisition [9, 13, 14, 18, 19]. In a mechanism akin to MHC II and CD1 molecules, we hypothesize that MR1 molecules internalized from the cell surface can be re-loaded with microbial antigens in the endosomal compartment and recycle to the cell surface to activate MR1-restricted T cells. Here we investigate the mechanisms underlying MR1 ligand exchange using a novel delivery method for MAIT cells antigens. We find that MR1 ligands are efficiently presented when delivered in the context of soluble MR1 molecules. This presentation is dependent on host MR1 and involves the transfer of antigen from the recombinant molecule onto MR1 protein expressed by the cell. Building upon our previously described tetraSPOT assay [20], this new method, the exSPOT, extends the tool box available to investigate MR1 biology and has provided important insights into the mechanisms of MR1-mediated antigen presentation.

Results

MR1 ligands delivered to antigen presenting cells on soluble MR1 molecules are efficiently recognized by MAIT cell clones

The MR1 ligand 5-OP-RU is inherently unstable in aqueous environments [11, 21], which presumably includes the intracellular milieu. However, the formation of a covalent bond with the lysine residue at position 43 of MR1 stabilizes the antigen [11]. We have successfully used such MR1/5-OP-RU complexes in their tetramerized form in plate-bound assays to activate MR1T cells [20]. Similarly, Priya and Brutkiewicz have used latex beads coated with MR1/5-OP-RU complexes to expand and activate human MAIT cells [22]. Thus, we hypothesized that recombinant MR1 proteins could also be used to stabilize and deliver 5-OP-RU in cell-based assays.

To test this hypothesis, we incubated human dendritic cells (DCs) with MR1 tetramers loaded with the canonical MAIT ligand 5-OP-RU (exSPOT), or bound the same concentration of tetramer directly to the ELISPOT plate prior to adding an MR1T cell clone (tetraSPOT). As expected based on previous work [20], the MR1T cells readily produced IFN-γ in the tetraSPOT, with an EC_{50} of 1.738 pM (Figure 1a). Intriguingly, in the exSPOT they also responded to DCs incubated with the same concentration of soluble MR1/5-OP-RU tetramers (Figure 1a). Indeed, the EC_{50} of tetramer in the presence of DCs decreased from 1.738 pM to 0.3767 pM ($p<0.0001$), representing a nearly five-fold increase in sensitivity compared to plate-bound tetramer. Interestingly, while MR1T cells did not respond to the MR1/6-FP tetramer in the tetraSPOT, we did observe some responses to the MR1/6-FP tetramers incubated with DCs at higher concentrations (Figure 1a). Similar to the tetraSPOT [20], MR1T cell activation by DCs incubated with soluble MR1 tetramers was dependent on MR1, as blocking with the anti-MR1 26.5 antibody markedly reduced the response (Figure 1b, EC_{50} of 0.94 pM *vs* 31.5 pM, $p<0.0001$).

As professional antigen presenting cells, DCs are particularly well equipped for phagocytosis of particulates of various sizes. To investigate whether such specific functionality was required in the exSPOT, we determined whether other cell types were capable of presenting ligand from

tetramers. We incubated the monocytic cell line THP-1, a B cell line (LCL), or the airway epithelial cell line BEAS-2B with MR1/5-OP-RU tetramers and quantified IFN-γ responses by an MR1T cell clone. As with DCs, the MR1T cell clone produced IFN-γ in response to all of the tetramer-incubated cell types (Figure 1c). However, DCs were nearly three orders of magnitude more efficient at presenting the antigen compared to the other cell types (EC_{50} of 0.55 pM *vs* 142 – 265 pM, $p<0.0001$).

Ligand delivered in the context of MR1 monomer is presented more efficiently than free ligand

Next, we compared the presentation of MR1/5-OP-RU tetramers and MR1/5-OP-RU monomers to reduce the complexity associated with any variability in the efficiency of biotinylation, streptavidin binding, and ligand saturation. Using the monomer, each MR1 protein delivered either one or no 5-OP-RU molecules whereas each MR1 tetramer might carry between zero and four 5-OP-RU molecules. Using the MR1 monomer further circumvented potential variability introduced by instability of the tetramer complex over time.

To our surprise, presentation of ligand from monomer-incubated DCs to MR1T cells was even more efficient than presentation of ligand from tetramer-incubated DCs (Figure 2a). Although the EC_{50} values of the complexes were comparable (Tetramer EC_{50}: 0.204 pM *vs* Monomer EC_{50}: 0.22 pM, $p=0.7486$), there was a marked difference in the estimated EC_{50} for 5-OP-RU which takes into account that each tetramer carries up to four 5-OP-RU molecules whereas each monomer carries one at most (Tetramer 5-OP-RU EC_{50}: 0.816 pM *vs* Monomer 5-OP-RU EC_{50}: 0.22 pM, $p<0.0001$). Comparing monomer-delivered 5-OP-RU to free ligand further revealed improved efficiency of the monomer over the unbound antigen (Figure 2a; Monomer EC_{50}: 0.22 pM *vs* Free EC_{50}: 4.97 pM, $p<0.0001$).

To further investigate the relative efficiency of loading free *vs* monomer-bound 5-OP-RU, we wanted to specifically detect MR1 molecules bearing 5-OP-RU at the cell surface by flow cytometry. To this end, we generated a TCR tetramer based on the TCR sequence of the same previously characterized MAIT cell clone that was used in the functional assays (D426-G11 – see

references [20, 23, 24]). We confirmed that this reagent specifically stained MR1 molecules loaded with 5-OP-RU but not 6-FP (Supplementary Figure 1). When we incubated BEAS-2B cells overexpressing GFP-tagged MR1 (BEAS-2B.MR1-GFP) with either MR1/5-OP-RU monomer or free 5-OP-RU overnight and stained with the TCR tetramer to track the cell surface translocation of MR1 bound to the antigen, almost 100-fold higher concentrations of free 5-OP-RU were needed to reach cell surface levels comparable to monomer-delivered ligand (Figure 2b+c). Together, these results demonstrate that soluble, recombinant MR1 is an efficient mechanism for delivery of MR1T cell ligands in a variety of cell lines *in vitro.*

Presentation of MR1 ligands delivered on soluble MR1 molecules requires host MR1

In principle, the MR1/5-OP-RU complex that interacts with the TCR in our assay could be either endogenously expressed MR1 bound to 5-OP-RU from the monomer or the recombinant MR1/5-OP-RU monomer itself. Thus, we tested whether endogenous MR1 was required. We incubated WT BEAS-2B cells, $MR1^{-/-}$ BEAS-2B cells lacking all isoforms of MR1, and $MR1^{-/-}$ BEAS-2B cells reconstituted with tetracycline-inducible MR1A [25, 26] with MR1/5-OP-RU monomer and used them as antigen presenting cells. As expected based on the results reported in Figure 1, we detected responses to WT BEAS-2B cells incubated with MR1/5-OP-RU monomers (Figure 3a, left). In contrast, when these monomers were incubated with the $MR1^{-/-}$ BEAS-2B cell line, the response was completely abrogated (Figure 3a, middle). Reconstitution of MR1 expression in the MR1-deficient cells resulted in complete recovery of MR1T cell responses to the monomer-delivered ligand (Figure 3a, right). These observations were confirmed in THP-1 cells (Figure 3b).

Soluble MR1 molecules are not detected at the cell surface

Having established that MR1 expression by the APC itself was required for presentation of monomer-delivered ligand, we considered two possible scenarios: (1) dimerization or indirect binding of the monomer to host MR1 at the cell surface and (2) uptake of the MR1/5-OP-RU complex and transfer of the antigen from the monomer onto the host MR1.

Since the MR1 molecules used to generate the ligand-loaded monomers and tetramers do not contain a transmembrane domain [11], their presence on the cell surface and, hence, ability to activate MR1T cells, would require lateral interactions with other membrane-bound proteins. Of note, Lion and colleagues have demonstrated that a GFP-tagged version of the MR1B isoform, which lacks the α3 domain [27], weakly associated with the MR1A isoform although that observation was considered a potential technical artifact [28]. To directly investigate the presence of the monomer on the cell surface, we incubated BEAS-2B.MR1-GFP cells with the biotinylated MR1/5-OP-RU monomer and stained the cells with fluorophore-coupled streptavidin. We did not detect any signal from the biotinylated monomer although our controls confirmed that we added sufficient monomer to induce MR1 surface translocation and sufficient streptavidin to detect biotinylated molecules at the cell surface (Figure 4). Interestingly, we detected a small but notable shift in total MR1 surface levels after incubation with the monomer (Figure 4, right). This suggests that enough 5-OP-RU ligand is delivered to increase not just TCR-reactive, but overall MR1 surface levels. While these results do not directly exclude the possibility, they do not provide any evidence for MR1 dimer formation at the cell surface, which could potentially allow the soluble MR1/5-OP-RU complexes to directly activate MR1T cells.

Ligands are exchanged from soluble MR1 molecules onto endogenous MR1

Since we could not find any evidence for direct presentation by the monomer, we next tested the hypothesis that the 5-OP-RU is transferred from the soluble MR1/5-OP-RU complex onto the MR1 expressed by the host cell. First, we sought to establish whether the MR1 expressed by the APC needed to be capable of presenting 5-OP-RU or whether its presence was sufficient. To investigate this, we reconstituted the MR1$^{-/-}$ BEAS-2B cell line with a CRISPR-resistant version of MR1A that carried the R9H mutation described by Howson et al. [29]. This mutation allows stable MR1 protein expression and binding of 6-FP but renders the protein incapable of presenting 5-OP-RU ([29] and Supplementary Figures 2 and 3). Indeed, reconstituting the MR1-deficient cells with this mutant did not rescue the presentation of either monomer-delivered 5-OP-RU or *M. smegmatis* supernatant (Figure 5a), further supporting the idea that it is the host MR1 that presents the 5-OP-RU ligand.

We reasoned that transfer of the 5-OP-RU molecule from the monomer onto the host MR1 is unlikely to occur at the cell surface as the probability of the ligand diffusing away would be too high. Instead, we hypothesized that the MR1/5-OP-RU complexes were actively internalized by the cell in an actin-dependent manner. To test whether the actin cytoskeleton was required, we treated BEAS-2B.MR1-GFP cells with latrunculin B (LatB), a well-characterized inhibitor of actin polymerization. Surface levels of 5-OP-RU-loaded MR1 were reduced in cells treated with LatB as compared to the DMSO control (Figure 5b). We concluded that an active, responsive actin cytoskeleton is required for presentation of the monomer-derived ligand. This is consistent with previous results demonstrating a requirement for actin for MR1 surface translocation in response to *Escherichia coli* (*E.coli*) [30] and could indicate a requirement for either internalization, lateral mobility or intracellular trafficking. While our experiment cannot discriminate between these interpretations, in conjunction with the surface staining experiment shown in Figure 4, a strong case can be made that the MR1 monomer is internalized.

To directly interrogate uptake of the recombinant MR1/5-OP-RU complex, we performed fluorescence microscopy. After 2 h, AlexaFluor647-labeled MR1 tetramer loaded with 5-OP-RU was clearly detectable within BEAS-2B cells counter-stained with the CellMask plasma membrane stain (Figure 5c). No AlexaFluor647 signal was detected in control cells without MR1 tetramer, confirming the specificity of the staining (Supplementary Figure 4).

Additional evidence for intracellular processing as opposed to cell surface exchange came from the observation that the kinetics of presentation differ between monomer-delivered ligand compared to free 5-OP-RU. Here, we incubated BEAS-2B.MR1-GFP cells with concentrations of MR1/5-OP-RU monomer (50 nM) and free 5-OP-RU (6.4 uM) that resulted in intermediate surface expression (Figure 2b+c) and followed MR1 surface translocation over time. In agreement with McWilliam et al., who detected surface expression of 5-OP-RU-loaded MR1 after 2 h [9], we saw loaded MR1 as soon as 1 h after addition of the free ligand (Figure 5d). By contrast, it took 2-4 h for the MR1 surface expression to reach comparable levels after addition of the MR1/5-OP-RU

monomer (Figure 5d). These kinetics are consistent with a longer time needed for internalization, processing, ligand exchange, and recycling of monomer-delivered ligand compared to free 5-OP-RU.

Exchange occurs in post-ER compartments and does not require acidification

Our data demonstrate the transfer of the monomer-delivered 5-OP-RU onto MR1 expressed by the APC but the mechanism of this exchange is unclear. Our lab has previously shown that pre-incubation with the non-stimulatory ligand 6-FP can increase MR1-mediated antigen presentation, presumably by increasing the pool of MR1 molecules available for ligand exchange in a post-ER compartment [13]. As expected from this, the presentation of *M. smegmatis* supernatant was more efficient after pre-incubation with 6-FP overnight (NaOH EC_{50}: 0.495 ul *vs* 6-FP EC_{50}: 0.059 ul, $p<0.0001$; Figure 6a, right). Importantly, when we applied this concept to the monomer delivery assay, we found a similar effect: releasing MR1 from the ER by pre-incubation with 6-FP decreased the EC_{50} for presentation of monomer-delivered ligand from 0.356 pM to 0.067 pM ($p<0.0001$; Figure 6a, left). Thus, MR1 molecules pre-loaded with a non-stimulating ligand appear to contribute to the activation of MR1T cells after delivery of antigenic ligand on monomers, supporting the notion of exchange. This also suggests that exchange of 5-OP-RU from the monomer onto the host MR1 is enhanced in post-ER compartments. In this context, it is worth noting that 6-FP concentrations multiple orders of magnitude higher were required to inhibit 5-OP-RU presentation in a functional assay [31], which suggests stronger binding of 5-OP-RU [9] and may help push the equilibrium towards binding of the activating ligand.

To probe to what extent the monomer delivery could be extended to other antigen presentation pathways and potentially gain mechanistic insights from any parallels, we repeated the assay with peptide-loaded MHC I and II tetramers. We first used a fluorophore-conjugated HLA-B*08:01/$CFP10_{3-11}$ tetramer to stain a $CD8^+$ T cell clone restricted by this MHC I/peptide complex (D480-F6 – see references [32] and [33]) for flow cytometry, confirming the T cell clone reacted with the tetramer (Figure 6b). However, using the same tetramer to load autologous DCs and using those cells in an ELISPOT with the same T cell clone did not result in the production of IFN-

γ in an APC-dependent manner (Figure 6c). As expected, the T cells responded to DCs incubated with free peptide (Figure 6c). Next, we tested an HLA-DRB1*14:03/ESAT6$_{73-78}$ tetramer in combination with a T cell clone that was specific to the antigen but restricted by a different MHC II allele (D481-D1, from an HLA-DRB1*14:03 negative individual). As expected, this tetramer did not stain the T cell clone by flow cytometry (Figure 6d). Nevertheless, feeding the non-matched tetramer to DCs autologous to the same MHC II-restricted T cell clone elicited an IFN-γ response (Figure 6e). The only source of matched MHC II molecules in this case are the DCs, further supporting a requirement for transfer of the antigen from the monomer onto antigen presenting molecules expressed by the APC itself as opposed to direct presentation of the monomer/antigen complex. In line with this, the T cells did not respond when using HLA-mismatched DCs or the A549 cell line which express MHC II alleles different from Donor 481 ([34], Cellosaurus cell line A-549 (CVCL_0023) (expasy.org)) (Figure 6f). Thus, like with MR1, presentation of the MHC II monomer-delivered peptide requires transfer onto proteins expressed by the APC itself.

Since monomers could efficiently deliver peptide for MHC II presentation, we reasoned that the MR1 loading in our assay was similar to the MHC II pathway, which involves exchange of a surrogate ligand in an endosomal compartment (reviewed e.g. in [7]). To test whether MR1 ligand transfer from the monomer could be mediated in an analogous fashion, we investigated the effect of brefeldin A (BFA) on the presentation of monomer-delivered 5-OP-RU. BFA disrupts the Golgi apparatus and effectively traps secretory proteins in the ER. Indeed, at steady-state, incubation with BFA diminished surface translocation of 5-OP-RU-loaded MR1 in response to the MR1/5-OP-RU monomer (Figure 6g, left). However, this experiment is unable to distinguish between two different scenarios: 1) ligand exchange occurs in the ER and MR1 needs to subsequently traverse the Golgi for surface presentation, or 2) MR1 needs to leave the ER to be available for exchange in a post-ER compartment. To distinguish between these two hypotheses, we pre-incubated the cells with 6-FP to induce ER egress of a pool of MR1 molecules before adding the BFA. Under these conditions, presentation of monomer-delivered ligand was unaffected (Figure 6g, second from left). It is important to note that BFA treatment also reduced total MR1 levels as measured by GFP expression (Figure 6g, right panels). BFA had a minimal

impact on GFP expression after pre-incubation with 6-FP, suggesting that ER egress protects MR1 from degradation. While these data do not preclude the possibility that ligand transfer can occur in the ER (provided that the MR1/5-OP-RU complex or free 5-OP-RU released from the monomer can reach it), they clearly show that 6-FP bound to cellular MR1 can be exchanged for 5-OP-RU derived from soluble monomer in a post-ER compartment.

Exchange of exogenous ligand onto MHC II [7, 35], CD1b [8] and CD1d [36-38] molecules is dependent on the low pH in the endolysosomal compartment. Pertinently, endosomal acidification is required for efficient presentation of *E.coli* by MR1 [16, 39] and McWilliam et al. have proposed that the Schiff base that links 5-OP-RU to the MR1 ligand binding groove is labile under acidic conditions [9, 19]. Therefore, we investigated whether presentation of monomer-delivered ligand was dependent on endosomal acidification using both a cell-free and a functional approach. First, we tested the stability of the MR1/5-OP-RU and MR1/6-FP monomers under increasingly acidic conditions in an ELISA. Fully folded, recombinant MR1 loaded with either 6-FP or 5-OP-RU was readily detectable using both a conformation-dependent anti-MR1 antibody [40] and an anti-$\beta_2$microglobulin (β_2m) antibody at neutral pH (Figure 7a). As expected, a control MHC I/peptide complex was detected by the anti-β_2m antibody but not by the anti-MR1 reagent. Since MR1 requires a ligand to efficiently refold *in vitro* [11, 41], both read-outs should specifically report on fully folded trimeric complexes. Surprisingly, binding of neither the anti-MR1 nor the anti-β_2m antibody was affected by overnight treatment of the plate-bound monomer with buffers of increasing acidity, covering the range of those observed in the endomembrane compartments (pH 4.5-7.5). Acidic conditions, therefore did not destabilize the antibody-reactive conformation of MR1 in this assay. Hence, it appears unlikely that loaded MR1 ligands are released simply by virtue of the acidic conditions in the endosomal compartment.

To confirm these results in a cellular assay, we pre-incubated BEAS-2B WT cells with bafilomycin before performing the exSPOT. Bafilomycin inhibits vacuolar ATPases [42] and impacts the presentation of an endosomal processing-dependent 5-A-RU pro-drug to MR1T cells [15]. Whereas the bafilomycin concentrations we used here reduced the MR1T cell response to this

pro-drug in a dose-dependent manner, presentation of the monomer-delivered 5-OP-RU was not affected by the inhibitor (Figure 7b). Together, these data support a model in which the transfer of 5-OP-RU delivered in the context of a soluble MR1 monomer onto the MR1 expressed by the APC occurs in a post-ER compartment, can displace pre-bound 6-FP, and is independent of endosomal acidification.

Discussion

Distinct and complementary cellular pathways have been proposed for MR1 loading and trafficking [14, 17-19]. While most research efforts have been focused on the ER pathway, increasing evidence supports exchange in a post-ER compartment as a mechanism by which MR1 acquires antigenic ligand(s). For example, both Karamooz et al. and McWilliam et al. have shown that MR1 molecules in cells pre-incubated with the MAIT cell antagonist 6-formylpterin (6-FP) can present activating MR1 ligands upon subsequent incubation with agonistic antigen [9, 13]. This exchange requires internalization of the molecules and partially counters the ability of Brefeldin A (BFA) to block surface expression of MR1/5-OP-RU complexes, indicating re-loading in a post-ER compartment [9]. Indeed, pre-incubation with 6-FP enhances MR1-mediated presentation of bacterial supernatant, presumably by increasing the pool of MR1 molecules available for re-loading in an endosomal compartment [13]. Using a fluorescence internalization probe (FIP), McWilliam et al. have directly demonstrated recycling of a small proportion of MR1 molecules in C1R cells [9]. In our model of mycobacterial infection of airway epithelial cells, this pathway contributes substantially to presentation of antigen derived from intracellular infection [12, 13].

A recently developed pro-drug requires endosomal processing to release the 5-OP-RU precursor 5-A-RU [15]. Since the antigen is generated in endosomes in this scenario, it appears likely that this compound is loaded onto MR1 in this compartment as opposed to trafficking to another intracellular organelle, which would require it to cross multiple membranes. Interestingly, while Ac-6-FP inhibits the presentation of free 5-A-RU, it does not interfere with the presentation of

this pro-drug [15]. This is consistent with the earlier observation that 6-FP blocks presentation of bacterial supernatant but not of intracellular infection [12]. Together, these results suggest that there are distinct pools of MR1 in the ER and in a post-ER compartment [14, 15, 17, 19], that these compartments are differentially accessed by exogenous ligands, and/or that conditions are more favorable for ligand exchange in the endosomal compartment than in the ER. This notion is not without precedent as multiple, complementary pathways including both direct loading in the ER and ligand exchange in the endosomal compartment have been shown for MHC I (reviewed e.g. in [43]).

Of note, a synthetic MR1 ligand modified to be able to track its location by microscopy resides in small vesicles also occupied by the micropinocytosis marker dextran 10 minutes post incubation [10]. This supports the idea that both membrane-bound internalized MR1 and soluble MR1 ligands could occupy this compartment at the same time, facilitating loading [19]. Furthermore, MR1-mediated antigen presentation of *M. smegmatis* supernatant is reduced upon knock-down of endosomal trafficking molecules [12, 13], further supporting involvement of this pathway in efficient antigen loading of some antigens.

In this study, we report a novel delivery method for MR1 ligands which allowed us to directly demonstrate transfer of the MR1T cell-activating ligand 5-OP-RU from recombinant, soluble MR1 onto cellular MR1. Intriguingly, monomer-delivered antigen was presented more efficiently than tetramer-delivered ligand. Considering the substantial difference in size, we speculate that monomeric protein may be internalized by a different mechanism and/or into a different compartment than tetramers. Alternatively, the bulky structure of the tetramer may result in steric hindrance of interactions with chaperones required for ligand transfer. The smaller, more compact monomer, on the other hand, may be better suited to adopt the correct orientation. Moreover, DCs were much more efficient at presenting the tetramer-derived ligand than other cell lines tested. In contrast to THP-1, LCL, and BEAS-2B cells, DCs are professional antigen presenting cells. Thus, the increased phagocytic ability of this specialized cell type may result in more efficient uptake of the soluble MR1, accounting for the enhanced presentation. Other

adaptations of professional APCs such as enhanced endolysosomal processing could also contribute to this phenotype.

Monomer-delivered 5-OP-RU was presented to MR1T cells more efficiently than free 5-OP-RU. One explanation for this observation is that binding to the monomer protects the inherently unstable antigenic molecule. However, the analogous results with MHC II tetramers argue that the enhanced antigen presentation associated with monomer delivery is not simply attributable to increased stability as peptide antigens are more stable. Therefore, we think it more likely that the monomer delivery enhances the efficiency of presentation by improving another aspect of antigen processing or presentation.

Our efforts to identify the molecular mechanism that enables transfer of the antigenic ligand from the soluble MR1 to the host MR1 show that this process is dependent on actin dynamics and can occur in a post-ER compartment. Peptide editing on MHC I and MHC II depends on the relative affinities of the available ligands and their competition for transiently ligand-receptive antigen presenting molecules [6, 7, 44]. Similarly, aGalCer variants on CD1d are only exchanged in the presence of a competing ligand [37]. In line with this concept, we propose that the endosomal compartment is a uniquely suited place for MR1 ligand exchange by virtue of its high local concentration of antigens derived from internalized pathogens relative to the cell as a whole. This enrichment of otherwise low abundance ligands may drive the equilibrium from pre-bound ligands to internalized antigens in endosomal compartments.

This analogy breaks down, however, in that neither peptides nor lipids are covalently bound to their antigen presenting molecules. By contrast, a covalent bond needs to be broken in our exchange assay to release the antigenic ligand from the soluble MR1. The Schiff base that anchors both 6-FP and 5-OP-RU to the MR1 binding groove is considered labile under acidic conditions [9, 19]. Nevertheless, our results suggest that ligand exchange on MR1 does not require endosomal acidification. While the exact molecular mechanism remains to be determined, this result leads us to propose that post-ER ligand exchange on MR1 is a facilitated process catalyzed by a yet

unidentified exchange chaperone. Monomer delivery may increase the efficiency of exchange by enhancing the interaction between pre-loaded MR1 and this chaperone. Indeed, specific chaperones facilitate the release of pre-loaded ligands, stabilize the transiently unoccupied antigen presenting molecule, and mediate the re-loading with antigenic cargo in other examples of post-ER ligand exchange. For MHC I, for example, this function can be fulfilled by TAPBPR in the Golgi (reviewed e.g. in [45] and [46]). For MHC II, HLA-DM chaperones endosomal ligand exchange and exchange kinetics are further modulated by its regulator HLA-DO (recently reviewed in [44] and [7]). Recent screens for modulators of MR1 loading and trafficking have identified numerous interaction partners through both genetic techniques and protein co-immunoprecipitation [10, 47]. These studies found MR1-mediated antigen presentation to be regulated by tapasin [10] and the P5-type ATPase ATP13A1 [47], but have largely focused on ER and Golgi-resident proteins. Discovery approaches more specifically targeted at interaction partners during ligand exchange may be needed to identify the chaperone(s) involved in this process. We postulate that modulation of the conformational flexibility of the MR1 binding groove will likely play an important role in ligand exchange as has been shown for MHC I, MHC II, and CD1d [38, 48, 49].

Previous evidence for exchange has been specific to exogenously added free ligand whereas presentation of antigen derived from intracellular mycobacterial infection was not boosted by pre-releasing MR1 proteins from the ER [13]. While this correlates with mechanistic differences [12, 13], it may also be related to what is the limiting factor in each scenario. In mycobacterial infections, the general abundance and/or local concentrations of antigenic ligand may be too low to tip the equilibrium towards exchange, even within the confines of the *Mycobacterium*-containing phagosome such that antigen and not MR1 is limiting. Exogenous addition of bacterial supernatant or purified MR1 ligands, in contrast, provides abundant antigen and the MR1 molecules available for exchange may become limiting. Hence, increasing the pool of post-ER MR1 has a direct impact on the magnitude of the response in this case. Similarly, monomer-delivered antigen provides an abundance of antigen, which makes this system responsive to changes in the post-ER MR1 levels.

In this manuscript, we explored the mechanisms by which MR1 ligands can be delivered exogenously using MR1 itself to stabilize an inherently unstable ligand. In addition to its use in exploring the molecular underpinnings of ligand exchange, we also postulate MR1/ligand complexes could be used as a vaccination strategy. In this instance, the highly conserved nature of MR1 is attractive as it reduces the risk of auto-antibody induction.

Methods

Human subjects

This study was conducted according to the principles expressed in the Declaration of Helsinki. Study participants, protocols, and consent forms were approved by the Institutional Review Board at Oregon Health & Science University (OHSU) (IRB00000186).

Cells and bacteria

M. smegmatis (strain mc^2155) supernatant was obtained by growing *M. smegmatis* and filtering the supernatant as described previously [13]. PBMCs were isolated from whole blood obtained by leukapheresis with informed consent, as previously described [50]. Human monocyte-derived dendritic cells (DCs) were isolated from PBMCs by plate adherence and cultured in RPMI+10% heat-inactivated (hi)-HuS with 30ng/ml GM-CSF (Immunex) and 10 ng/ml IL-4 (R&D Systems) as previously described [51]. BEAS-2B cells were obtained from the American Type Culture Collection (ATCC) and cultured as recommended. BEAS-2B $MR1^{-/-}$, BEAS-2B $MR1^{-/-}$: MR1A cell lines were described previously [25, 26]. The BEAS-2B cell line overexpressing GFP-tagged MR1A (BEAS-2B.MR1-GFP) was described previously [12]. THP-1 cells were obtained from ATCC. THP-1 $MR1^{-/-}$ and THP-1 $MR1^{-/-}$: MR1 cell lines were described previously [26, 52]. The THP-1 $MR1^{-/-}$ from the Sewell lab constitutively express Cas9 protein whereas the THP-1 $MR1^{-/-}$: MR1 cells from the Cerundolo lab do not. EBV-transformed B cell lines (LCL) were generated in our laboratory using supernatants from the cell line 9B5–8 (ATCC). A549 cells were obtained from

ATCC. The MR1 R9H res construct was based on [29]. MR1 res and MR1 R9H res contain silent mutations to make the sequence resistant to CRISPR/Cas9 editing in the MR1$^{-/-}$ background. The coding sequence with a downstream IRES GFP [53] was ordered from GeneArt (ThermoFisher) and cloned into our previously described pCI AscI vector [13]. Plasmids were sequenced at the OHSU sequencing core and transfected into BEAS-2B MR1$^{-/-}$ cells using the Amaxa nucleofection system with Kit T solution (Lonza). The transfection efficiency was evaluated via GFP expression by flow cytometry (Supplementary Figure 3). *Trichoplusia ni* (Hi-5) and *Spodoptera fugiperda* cells (Sf9) cells for baculovirus production and recombinant protein expression maintained as described previously [54].

T cell clones

All T cell clones were expanded and maintained as previously described [23, 32]. Three T cell clones were used in this work. Two clones have been published previously (D426-G11 [20, 23] and D480-F6 [32, 33]). D481-D1 is a CD4^{+} T cell clone that recognizes Esat6$_{73-87}$. This clone was generated in a limiting dilution assay by adding either 100, 200 or 600 CD4^{+} T cells (CD4 microbeads, Miltenyi) isolated from PBMC from D481, a participant who had active tuberculosis, to wells of a 96 well plate containing 1e5 irradiated (3,500 rad using a Cs source) allogeneic PBMCs, 1e4 irradiated (3,500 rad using a Cs source) autologous dendritic cells (prepared as described above), 2ug/ml Esat6 protein (BEI Resources), 5ng/ml interleukin-2 (Proleukin) and incubated at 37°C for two weeks. Wells with growth were assessed for function to an Esat6 peptide pool consisting of 15mers overlapping by 11 amino acids in an IFN-γ ELISPOT. T cell clones that responded to Esat6 peptide pool were expanded as described previously [23, 32] and further screened against the individual 15mers from the Esat6 peptide pool. The restricting allele is not known for this clone, but D481 expresses these class II alleles: DRB1*08:01, DRB1*13:01, DPB1*01:01, DPB1*04:01, DQB1*04:02 and DQB1*06:03 (HLA typing by Kashi Clinical Laboratories, Portland, OR).

ELISPOT assays

For the plate-bound tetramer ELISPOT (tetraSPOTetraSPOT) assay, ELISPOT plates were coated with an anti–IFN-γ antibody, as previously described (Heinzel 2002 HLA-E). At the time of coating, MR1/5-OP-RU and MR1/6-FP tetramers conjugated to PE obtained from the NIH tetramer core [11] were added at a range of concentrations. After overnight incubation at 4°C, ELISPOT plates were washed three times with phosphate-buffered saline and then blocked with RPMI 1640 + 10% human serum for at least 1 hour. T cell clones (1e3-2e4) were added to wells overnight. IFN-γ ELISPOTs were enumerated following development as previously described [55]. For all other ELISPOT assays, ELISPOT plates were coated with anti-IFN-γ antibody and blocked as described above. 1e4 DC, LCL, THP-1 or BEAS-2B cells were plated in the ELISPOT wells in RPMI+10% HuS. Tetramer, monomer, ligand or peptide were added to the wells at concentrations indicated for each experiment. PHA was used as positive control. After at least one hour, 1e3-2e4 T cell clones were added and the plate was incubated overnight at 37°C. 6-FP pre-treatment assays were performed as described [13]. Briefly, BEAS-2B.MR1-GFP cells were plated in 6-well tissue culture plates and treated with 6-FP *vs* NaOH control. After 16 h, the cells were harvested and used as APCs in an IFN-γ ELISPOT assay as described above. For experiments with Bafilomycin A1 (BAFA1, MedChemExpress), BEAS-2B cells were incubated with BAFA1 for 2 h at indicated concentrations prior to the addition of 100 pM MR1/5-OP-RU monomer or 50 nM 5-OP-RU prodrug (MedChemExpress) in an IFN-γ ELISPOT assay as described above.

5-OP-RU Ligand

5-(2-oxopropylideneamino)-6-d-ribitylaminouracil (5-OP-RU) was made from two sources of 5-amino-6-D-ribitylaminouracil (5-A-RU). For the first method, 5-nitro-6-d-ribitylaminouracil (5-N-RU) was prepared by the OHSU Medicinal Chemistry Core. 5-A-RU was freshly prepared from 5-N-RU following a previously described procedure [11]. In brief, 4.8 mg of 5-N-RU was dissolved in 400 ul 50 mM MES, pH 5.8. 8-fold molar excess of sodium dithionite powder was added and incubated in the dark at 90°C for five minutes under argon. The solution was chilled in an ice water bath. To prepare 5-OP-RU, at least 33 molar equivalents of methylglyoxal was added to 5-A-RU in 100 mM HEPES, pH 7.2, 150 mM NaCl to give a stock solution at 20 mM. For the second method, 5-A-RU*HCl was prepared by the OHSU Medicinal Chemistry Core following a previously

described procedure [56]. To prepare 5-OP-RU, 5 ul of circa 650 mM methylglyoxal (Sigma) was added to 5 ul of 32 mM 5-A-RU*HCl dissolved in water immediately before addition to the assay to give a stock solution of 16 mM of 5-OP-RU.

Flow Cytometry assays

The following reagents were obtained through the NIH Tetramer Core Facility: MR1/5-OP-RU tetramer and monomer and MR1/6-FP tetramer and monomer, HLA*B08:01/CFP10$_{3-11}$ tetramer, HLA-DRB1*14:03/Esat6$_{73-87}$ tetramer, HLA-DRB1*14:03/control tetramer. Identification of MAIT cells with MR1 tetramers was described in [11]. The D426-G11 TCR tetramer was made as specified below. To confirm the specificity of the TCR tetramer as a staining reagent, BEAS-2B.MR1-GFP cells were incubated with the indicated concentrations of 5-OP-RU or 6-FP, or the equivalent volume of 0.01 M NaOH overnight. Cells were harvested with Trypsin and split into three wells of a U-bottom 96-well plate each for staining with TCR tetramer, anti-MR1 antibody 26.5 (BioLegend, 361108), or isotype control antibody (BioLegend, 400222) for at least 30 min on ice. BEAS-2B MR1-/- cells transfected with the MR1 res or MR1 R9H res plasmids were analyzed similarly. For ligand titration experiments, 5e4 BEAS-2B.MR1-GFP cells per well were incubated with the indicated concentrations of free 5-OP-RU or MR1/5-OP-RU monomer in a 24-well plate overnight. Cells were harvested with Trypsin, transferred to a 96-well U-bottom plate, washed, and stained with TCR tetramer for at least 30 min on ice. Free ligand and monomer titrations were performed in parallel. For time course experiments, 5e4 BEAS-2B.MR1-GFP cells per well were plated in 12 or 24-well plates. Free 5-OP-RU or MR1/5-OP-RU were added to the indicated final concentrations for the indicated amounts of time. Samples from all time points were harvested and stained at the same time as above but incubated with TCR tetramer at RT. Free ligand and monomer time courses were performed on separate days. For the actin blockade, 5e4 BEAS-2B.MR1-GFP cells were plated in 24-well plates and left to adhere overnight. Cells were then treated with 10 uM Latrunculin B (Sigma, 428020-1MG) or the equivalent volume of DMSO (Sigma, D2650-100ML). After 1 h, MR1/5-OP-RU or MR1/6-FP monomer was added to a final concentration of 100 nM and the cells were incubated for another 4 h before staining as above. For Brefeldin A blocking experiments, BEAS-2B.MR1-GFP cells were incubated with 94 uM 6-

formylpterin (6-FP, Schricks, 11425-100) or the equivalent volume of 0.01 M NaOH (Sigma, MKCC6914) overnight at 37°C at 5e4/well in a 24-well plate. 6-FP was washed off and the cells treated with Brefeldin A (BFA, Sigma, B5936-200UL) or the equivalent volume of DMSO (Sigma, D2650) for one hour, followed by the addition of MR1/6-FP or MR1/5-OP-RU monomer (100nM) and incubation at 37°C for four hours. Cells were then stained with TCR tetramer as above. TCR tetramer was used at 150 or 300 nM. BEAS-2B WT cells were used for unstained and single color controls. Anti-MHC I antibody W6/32 (BioLegend, 311410) was used for the APC single color control due to low MR1 expression on BEAS-2B WT cells. For surface staining of BEAS-2B.MR1-GFP cells with streptavidin, 3e5 cells were incubated with 50 nM of MR1/5-OP-RU monomer or medium overnight. These cells were split into multiple wells and either stained with the TCR tetramer as described above or blocked with PBS + goat, human, and bovine serum for at least 30 min on ice and then stained with Streptavidin-APC (Agilent, PJ27S-1) for 40 min on ice or with biotinylated anti-MR1 antibody 26.5 for 40 minutes on ice, followed by Steptavidin-APC for 40 minutes on ice. For tetramer staining of the CD8 T cell clone D480-F6, 1e5 T cell clones were incubated with the HLA*B08:01/CFP10$_{3-11}$ tetramer at 1:500 (0.127 ug/well) for 45 minutes at 37°C. For tetramer staining of the CD4 T cell clone D481-D1, 1e5 T cell clones were incubated with the HLA-DRB1*14:03/Esat6$_{73-87}$ or HLA-DRB1*14:03/control at 6 ug/ml for 1 hour at 37°C. Cells were then subsequently stained with an antibody cocktail containing LIVE/DEAD Fixable Dead Cell Stain Kit (Thermo Fisher), and surface stained with the antibodies to CD4 (BD Biosciences, clone SK3 348789), CD8 (Biolegend, clone SK1344714), and CD3 (BD Biosciences, clone SK7340663), for 30 minutes at 4°C. Samples were washed and fixed with 1% PFA. Acquisition was performed using a BD FACSymphony, LSRII, or Canto cytometer. Flow cytometric analysis was performed using FlowJo version 10.6.1 or 10.7.1 (Treestar, Ashland, OR, USA). Plots show GFP+ gates to ensure only cells over-expressing MR1 are included in the analysis.

Recombinant protein expression and purification

The D426-G11 TCR was produced as previously described for other MAIT TCRs [57]. Briefly, the D426-G11 TCR V(D)J region of each TCR chain was cloned separately into the pAcGP67a vector after the GP67 signal sequence and before either a “cysteine-optimized” TRAC or TRBC

sequence [58]. To ensure heterodimer formation, the chains were tagged with cleavable C-terminal acidic and basic zippers [59]each followed with a 6xHis tag. The alpha chain construct contained a C-terminal AviTag before the zipper cleavage site. The P1 and P2 baculoviruses were produced in Sf9 cells[54], then the baculoviruses were added in tandem to Hi-5 cells and the cells were allowed to express the recombinant protein for 72 hours. The supernatant was harvested and the protein purified by Ni-NTA chromatography. Recombinant TCR was then treated with recombinant HRV 3C protease overnight and the cleaved zippers were removed with Ni-NTA. The protein was biotinylated *in vitro* using recombinant BirA ligase and the biotinylation efficiency checked by a streptavidin gel-shift assay. Finally, it was purified by size exclusion chromatography and tetramerized with streptavidin-APC (Agilent PJ27S).

Microscopy

BEAS-2B cells (1e5) were seeded on a chamber slide and incubated for 18 h at 37C. MR1/5-OP-RU tetramer conjugated to AF647 (200nM) was added to the experimental wells for 2 h at RT. Control wells received no tetramer. All cells then had CellMask Orange Plasma (1:5000 dilution, Invitrogen) added for 10 min before DAPI was added and cells were washed 2X in PBS. Images were acquired on a Keyence BZ-X810 Flourescence microscope. And all images acquired were using the same microscope settings.

Cell-free acidification assay

In addition to MR1/5-OP-RU and MR1/6FP from the NIH Tetramer Core, recombinant, biotinylated γδ TCR ("DP10.7") [60] and HLA-A2:MART-1 [61] were made in-house as previously described and used as controls for this ELISA assay. Extensive washing with PBS pH 7.4 + 0.5% Tween-20 was performed between each step/treatment outlined below. First, traptavidin, a variant of streptavidin with a slower biotin off-rate [62], was immobilized on an ELISA plate in 0.1 M Na_2CO_3, pH 9.6 overnight. The plate was blocked with 0.5% BSA in 1xPBS, then biotinylated MR1, TCR, and HLA-A2 were immobilized as appropriate. Eight working buffers of 1xPBS were made from a house-made 10xPBS stock spanning pH 4.6-7.4. Protein was treated with either PBS

pH 7.4 (controls) or PBS of variable pH overnight at 4C. (This experiment was also performed with a citrate-phosphate buffer system, which unlike PBS, has a buffering range spanning the experimental conditions, and the results did not differ from those using PBS, which has a buffering range of ~5.8-7.4 pH units.) After removal of the acidic buffer and washing with PBS pH 7.2, either anti-human MR1 (unlabeled, clone 26.5, BioLegend 361102) or anti-human B2m (unlabeled, clone B2M-01, Novus Biologicals NB500-317) antibody was applied to the plate, followed by a rabbit anti-mouse IgG H+L, HRP-conjugated secondary antibody (Abcam ab6728). The ELISA was developed with a TMB substrate kit (Thermo Scientific 34021) and the absorbance was detected at 450 nm using a Tecan Safire 2 plate reader.

Data analysis and Statistics

Data were analyzed with Prism 9 GraphPad Software. For measurements of functional avidity, curves were determined by non-linear regression and best-fit EC_{50} was calculated. EC_{50} values were compared with the extra sum-of-squares F test.

Data Availability

The authors declare that the data supporting the findings of this study are available within the paper and its supplementary information files.

Acknowledgements

We would like to thank the participants who gave time and dedication to this health research as well as Erin Merrifield, Department of Pediatrics, OHSU, for her contributions to this study.

This project has been funded in whole or in part with Federal funds from the National Institutes of Allergy and Infectious Diseases, National Institutes of Health, Department of Health and Human Services, under grant no AI147954 (EA, DML), AI134790 (DML), GM007183 (NAL) and AI129976 (MH). This work was also supported in part by Merit Award #I01 CX001562 from the U.S. Department of Veterans Affairs Clinical Sciences Research and Development Program (MJH),

Merit Award #I01 BX000533 from the U.S. Department of Veterans Affairs Biomedical Laboratory (DML).

Author Contributions

CK, GS, NAL, DAL, EJA, DML and MH contributed to the conception and/or design of the work. CK and GS are joint first authors. DML and MH jointly supervised the work. MC, MN, DAL and DML contributed to clinical activities. EJA, DML and MH raised grants to fund the research. CK, GS, NAL, MC, MN, AW, CL, TA, JB, DAL, EJA, DML and MH substantially contributed to the acquisition, analysis, or interpretation of data and drafting of the manuscript. All authors substantially contributed to revising and critically reviewing the manuscript for important intellectual content. All authors approved the final version of this manuscript to be published and agree to be accountable for all aspects of the work.

Figure Legends

Fig 1. MR1 ligands delivered to antigen presenting cells on soluble MR1 molecules are efficiently recognized by MAIT cell clones. A. MAIT clone (1e4) IFN-γ responses to MR1/5-OP-RU or MR1/6-FP tetramer, either added to dendritic cells (1e4) or bound to ELISPOT plate (tetraSPOT). EC_{50} calculated using non-linear regression and the difference in the EC_{50} was statistically significant between the curves ($p<0.0001$) by the extra sum-of-squares F test. B**.** MR1T clone (1e4) IFN-γ response to MR1/5-OP-RU is inhibited by anti-MR1 antibody blockade (2ug/ml). Data are representative of three independent experiments. **C**. MR1T clone (1e4) IFN-γ response to MR1/5-OP-RU tetramer, added to either DCs, THP-1 cells, BEAS-2B (B2B) cells or B-LCL (1e4). EC_{50} calculated using non-linear regression and the difference in the EC_{50} was statistically significant between the curves ($p<0.0001$) by the extra sum-of-squares F test. Error bars denote standard deviation.

Fig 2. Ligand delivered in the context of MR1 monomer is presented more efficiently than free ligand. A. MR1T clone (1e4) IFN-γ response to MR1/5-OP-RU tetramer, MR1/5-OP-RU monomer, and soluble 5-OP-RU. Concentration of 5-OP-RU calculated for tetramer and monomer and EC_{50} calculated using non-linear regression for IFN-γ response to the concentration of 5-OP-RU. The difference in the EC_{50} was statistically significant between the MR1/5-OP-RU tetramer and 5-OP-RU and between MR1/5-OP-RU monomer and 5-OP-RU curves ($p<0.0001$), but there was no significant difference in the EC_{50} of MR1/5-OP-RU tetramer and monomer by the extra sum-of-squares F test ($p=0.7486$). Error bars denote standard deviation.

B+C., BEAS-2B.MR1-GFP cells were incubated with the indicated concentrations of MR1/5-OP-RU monomer or free 5-OP-RU overnight and surface stained for flow cytometry with APC-conjugated TCR tetramer.
Data are representative of three (**A**) and four (**B**) independent experiments.

Fig 3. Presentation of MR1 ligands delivered on soluble MR1 molecules requires host MR1. A. MR1T clone (1e3) IFN-γ response to BEAS-2B, BEAS-2B MR1$^{-/-}$ and BEAS-2B MR1$^{-/-}$: MR1A (1e4) incubated with MR1/5-OP-RU or MR1/6-FP monomers. Also included in MR1T clone IFN-γ response to MR1/5-OP-RU tetramer only with no antigen presenting cells. **B.** Same as **A.**, except the antigen presenting cells are THP-1, THP-1 MR1$^{-/-}$ and THP-1 MR1$^{-/-}$: MR1A (1e4). Data are representative of two independent experiments. Error bars denote standard deviation.

Fig 4. Soluble MR1 molecules are not detected at the cell surface.
BEAS-2B.MR1-GFP cells (3e5) were pre-incubated with 50 nM of MR1/5-OP-RU monomer overnight before staining with either Streptavidin (left), TCR tetramer (middle) or biotinylated 26.5 anti-MR1 antibody followed by Streptavidin (right). The same unstained and primary antibody only controls are shown the left and right panels for easy comparison. Data are representative of three independent experiments.

Fig 5. Ligands are exchanged from the soluble MR1 molecules onto endogenous MR1.
A. MR1T clone (1e3) IFN-γ response to BEAS-2B MR1$^{-/-}$ cells (1e4) that had been transfected with the MR1 or MR1 R9H plasmid, followed by addition of the MR1/5-OP-RU monomer, or 1μL of *M. smegmatis* supernatant. Error bars denote standard deviation.
B. BEAS-2B.MR1-GFP cells were pre-incubated with 10 uM of latrunculin B (LatB) for 1 h before addition of MR1/5-OP-RU or MR1/6-FP monomer for an additional 4 h. Cells were surface stained with TCR tetramer.
C. BEAS-2B cells (1e5) were seeded in a chamber slide and incubated for 18 h at 37C. MR1/5-OP-RU tetramer conjugated to AF647 (200nM) was added for 2 h at RT. All cells then had CellMask Orange Plasma (1:5000 dilution, Invitrogen) added for 10 min before DAPI was added and cells were washed 2X in PBS.
D. BEAS-2B.MR1-GFP cells were incubated with either 50 nM MR1/5-OP-RU monomer or 6.4 uM of free 5-OP-RU for indicated amounts of time before surface staining for flow cytometry with TCR tetramer. Monomer and free ligand time courses were performed as separate experiments. Data are representative of three (**A**, **B**, **D**) and three (**C**) independent experiments.

Fig 6. Exchange occurs in post-ER compartments. A. MR1T clone (1e4) IFN-γ response to BEAS-2B.MR1-GFP (1e4) that were pretreated with 6-FP *vs* control using *M. smegmatis* supernatant or MR1/5-OP-RU monomer as the antigen. EC_{50} calculated using non-linear regression and the difference in the EC_{50} was statistically significant between the curves ($p<0.0001$) by the extra sum-of-squares F test.
B. D480-F6 T cell clone was stained with the HLA-B*08:01 tetramer to $CFP10_{3-11}$, along with antibodies to CD3, CD4, CD8 and a live/dead discriminator. Live, $CD3^{+}CD4^{-}CD8^{+}$ T cells are shown.
C. D480-F6 T cell clone (5e3) IFN-γ response to dendritic cells (1e4) that were incubated with

either the $CFP10_{3-11}$ tetramer or $CFP10_{3-11}$ peptide. 9.5e4 irrelevant T cells (D426G11) were also added to the well to decrease T:T presentation of classical T cell clone.
D. D481-D1 T cell clone was stained with the HLA-DRB1*14:03 tetramer to $Esat6_{73-87}$ or a control tetramer along with antibodies to CD3, CD4, CD8 and a live/dead discriminator. Live, $CD3^+CD8^-CD4^+$ T cells are shown.
E. D481-D1 T cell clone (2e4) IFN-γ response to D481 (autologous) dendritic cells (2e4) that were incubated with either the $Esat6_{73-87}$ tetramer, control tetramer or $Esat6_{73-87}$ peptide.
F. D481-D1 T cell clone (2e4) IFN-γ response to D481 (autologous) dendritic cells, D520 mismatched dendritic cells or A549 cells (2e4) that were incubated with the $Esat6_{73-87}$ tetramer.
G. BEAS-2B.MR1-GFP cells were pre-incubated with 6-FP or NaOH overnight. 6-FP was washed off and cells were incubated with 50 ug/ml brefeldin A (BFA) for 1h before addition of MR1/5-OP-RU or MR1/6-FP monomer for an additional 4 h. Cells were surface stained for flow cytometry with TCR tetramer.
Data are representative of three (**A**, **D** - **G**) or two (**B**, **C**) independent experiments. Error bars denote standard deviation.

Fig. 7. Exchange does not require acidification.
A. Biotinylated MR1 monomer, recombinant TCR, or HLA-A2 were immobilized on a traptavidin-coated plate before incubation with PBS at the indicated pH overnight at 4C. Binding of either anti-MR1 (clone 26.5) or anti-b2m (clone B2M-01) antibody was assess with an HRP-conjugated secondary antibody and TMB substrate. Error bars denote standard deviation.
B. MR1T clone (5e3) IFN-γ response to BEAS-2B (1e4) pre-treated with Bafilomycin A1 for 2 hours, followed by addition of the MR1/5-OP-RU monomer or 5-OP-RU prodrug. Data in **B** are representative of three independent experiments.

References

1. Godfrey, D.I., et al., *The biology and functional importance of MAIT cells.* Nat Immunol, 2019. **20**(9): p. 1110-1128.
2. Hinks, T.S.C. and X.W. Zhang, *MAIT Cell Activation and Functions.* Front Immunol, 2020. **11**: p. 1014.
3. Toubal, A., et al., *Mucosal-associated invariant T cells and disease.* Nat Rev Immunol, 2019. **19**(10): p. 643-657.
4. Chiba, A., G. Murayama, and S. Miyake, *Characteristics of mucosal-associated invariant T cells and their roles in immune diseases.* Int Immunol, 2021. **33**(12): p. 775-780.
5. Crowther, M.D. and A.K. Sewell, *The burgeoning role of MR1-restricted T-cells in infection, cancer and autoimmune disease.* Curr Opin Immunol, 2021. **69**: p. 10-17.
6. Trowitzsch, S. and R. Tampé, *Multifunctional Chaperone and Quality Control Complexes in Adaptive Immunity.* Annual Review of Biophysics, 2020. **49**(1): p. 135-161.
7. Alvaro-Benito, M. and C. Freund, *Revisiting nonclassical HLA II functions in antigen presentation: Peptide editing and its modulation.* HLA, 2020. **96**(4): p. 415-429.

8. Moody, D.B. and R.N. Cotton, *Four pathways of CD1 antigen presentation to T cells.* Curr Opin Immunol, 2017. **46**: p. 127-133.
9. McWilliam, H.E., et al., *The intracellular pathway for the presentation of vitamin B-related antigens by the antigen-presenting molecule MR1.* Nat Immunol, 2016. **17**(5): p. 531-7.
10. McWilliam, H.E.G., et al., *Endoplasmic reticulum chaperones stabilize ligand-receptive MR1 molecules for efficient presentation of metabolite antigens.* Proc Natl Acad Sci U S A, 2020. **117**(40): p. 24974-24985.
11. Corbett, A.J., et al., *T-cell activation by transitory neo-antigens derived from distinct microbial pathways.* Nature, 2014. **509**(7500): p. 361-5.
12. Harriff, M.J., et al., *Endosomal MR1 Trafficking Plays a Key Role in Presentation of Mycobacterium tuberculosis Ligands to MAIT Cells.* PLoS Pathog, 2016. **12**(3): p. e1005524.
13. Karamooz, E., et al., *MR1 recycling and blockade of endosomal trafficking reveal distinguishable antigen presentation pathways between Mycobacterium tuberculosis infection and exogenously delivered antigens.* Scientific Reports, 2019. **9**(1): p. 4797.
14. Kulicke, C., et al., *Covering All the Bases: Complementary MR1 Antigen Presentation Pathways Sample Diverse Antigens and Intracellular Compartments.* Frontiers in Immunology, 2020. **11**.
15. Lange, J., et al., *The Chemical Synthesis, Stability, and Activity of MAIT Cell Prodrug Agonists That Access MR1 in Recycling Endosomes.* ACS Chemical Biology, 2020.
16. Ussher, J.E., et al., *TLR signaling in human antigen-presenting cells regulates MR1-dependent activation of MAIT cells.* European Journal of Immunology, 2016. **46**(7): p. 1600-1614.
17. Karamooz, E., M.J. Harriff, and D.M. Lewinsohn, *MR1-dependent antigen presentation.* Seminars in Cell & Developmental Biology, 2018. **84**: p. 58-64.
18. Lamichhane, R. and J.E. Ussher, *Expression and trafficking of MR1.* Immunology, 2017. **151**(3): p. 270-279.
19. McWilliam, H.E.G. and M. Salio, *Understanding and modulating the MR1 metabolite antigen presentation pathway.* Molecular Immunology, 2021. **129**: p. 121-126.
20. Harriff, M.J., et al., *MR1 displays the microbial metabolome driving selective MR1-restricted T cell receptor usage.* Sci Immunol, 2018. **3**(25).
21. Mak, J.Y., et al., *Stabilizing short-lived Schiff base derivatives of 5-aminouracils that activate mucosal-associated invariant T cells.* Nat Commun, 2017. **8**: p. 14599.
22. Priya, R. and R.R. Brutkiewicz, *MR1 Tetramer-Based Artificial APCs Expand MAIT Cells from Human Peripheral Blood That Effectively Kill Glioblastoma Cells.* Immunohorizons, 2021. **5**(6): p. 500-511.
23. Gold, M.C., et al., *Human mucosal associated invariant T cells detect bacterially infected cells.* PLoS Biol, 2010. **8**(6): p. e1000407.
24. Gold, M.C., et al., *MR1-restricted MAIT cells display ligand discrimination and pathogen selectivity through distinct T cell receptor usage.* J Exp Med, 2014. **211**(8): p. 1601-10.
25. Narayanan, G.A., et al., *Alternative splicing of MR1 regulates antigen presentation to MAIT cells.* Sci Rep, 2020. **10**(1): p. 15429.
26. Salio, M., et al., *Ligand-dependent downregulation of MR1 cell surface expression.* Proc Natl Acad Sci U S A, 2020. **117**(19): p. 10465-10475.

27. Riegert, P., V. Wanner, and S. Bahram, *Genomics, isoforms, expression, and phylogeny of the MHC class I-related MR1 gene.* J Immunol, 1998. **161**(8): p. 4066-77.
28. Lion, J., et al., *MR1B, a natural spliced isoform of the MHC-related 1 protein, is expressed as homodimers at the cell surface and activates MAIT cells.* Eur J Immunol, 2013. **43**(5): p. 1363-73.
29. Howson, L.J., et al., *Absence of mucosal-associated invariant T cells in a person with a homozygous point mutation in MR1.* Sci Immunol, 2020. **5**(49).
30. Salerno-Goncalves, R., T. Rezwan, and M.B. Sztein, *B cells modulate mucosal associated invariant T cell immune responses.* Front Immunol, 2014. **4**: p. 511.
31. Eckle, S.B., et al., *A molecular basis underpinning the T cell receptor heterogeneity of mucosal-associated invariant T cells.* J Exp Med, 2014. **211**(8): p. 1585-600.
32. Lewinsohn, D.A., et al., *Immunodominant tuberculosis CD8 antigens preferentially restricted by HLA-B.* PLoS Pathog, 2007. **3**(9): p. 1240-9.
33. Lancioni, C., et al., *Recognition of CD8(+) T-cell epitopes to identify adults with pulmonary tuberculosis.* Eur Respir J, 2019. **53**(5).
34. Adams, S., et al., *HLA class I and II genotype of the NCI-60 cell lines.* J Transl Med, 2005. **3**(1): p. 11.
35. Freund, C. and T. Hofer, *A Missing Switch in Peptide Exchange for MHC Class II Molecules.* Front Immunol, 2019. **10**: p. 2513.
36. Chen, X., et al., *Distinct endosomal trafficking requirements for presentation of autoantigens and exogenous lipids by human CD1d molecules.* J Immunol, 2007. **178**(10): p. 6181-90.
37. Bai, L., et al., *Lysosomal recycling terminates CD1d-mediated presentation of short and polyunsaturated variants of the NKT cell lipid antigen alphaGalCer.* Proc Natl Acad Sci U S A, 2009. **106**(25): p. 10254-9.
38. Cuevas-Zuviria, B., et al., *Dynamic plasticity of the lipid antigen-binding site of CD1d is crucially favoured by acidic pH and helper proteins.* Sci Rep, 2020. **10**(1): p. 5714.
39. Le Bourhis, L., et al., *Antimicrobial activity of mucosal-associated invariant T cells.* Nat Immunol, 2010. **11**(8): p. 701-8.
40. Huang, S., et al., *Evidence for MR1 antigen presentation to mucosal-associated invariant T cells.* J Biol Chem, 2005. **280**(22): p. 21183-93.
41. Kjer-Nielsen, L., et al., *MR1 presents microbial vitamin B metabolites to MAIT cells.* Nature, 2012. **491**(7426): p. 717-23.
42. Bowman, E.J., A. Siebers, and K. Altendorf, *Bafilomycins: a class of inhibitors of membrane ATPases from microorganisms, animal cells, and plant cells.* Proc Natl Acad Sci U S A, 1988. **85**(21): p. 7972-6.
43. Blander, J.M., *Regulation of the Cell Biology of Antigen Cross-Presentation.* Annu Rev Immunol, 2018. **36**: p. 717-753.
44. Sadegh-Nasseri, S., *Partnering for the major histocompatibility complex class II and antigenic determinant requires flexibility and chaperons.* Curr Opin Immunol, 2021. **70**: p. 112-121.
45. Hafstrand, I., A. Aflalo, and L.H. Boyle, *Why TAPBPR? Implications of an additional player in MHC class I peptide presentation.* Current Opinion in Immunology, 2021. **70**: p. 90-94.

46. Thomas, C. and R. Tampe, *MHC I assembly and peptide editing - chaperones, clients, and molecular plasticity in immunity.* Curr Opin Immunol, 2021. **70**: p. 48-56.
47. Kulicke, C.A., et al., *The P5-type ATPase ATP13A1 modulates major histocompatibility complex I-related protein 1 (MR1)-mediated antigen presentation.* J Biol Chem, 2022. **298**(2): p. 101542.
48. Natarajan, K., et al., *The Role of Molecular Flexibility in Antigen Presentation and T Cell Receptor-Mediated Signaling.* Front Immunol, 2018. **9**: p. 1657.
49. Wieczorek, M., et al., *Major Histocompatibility Complex (MHC) Class I and MHC Class II Proteins: Conformational Plasticity in Antigen Presentation.* Front Immunol, 2017. **8**: p. 292.
50. Lewinsohn, D.M., et al., *Mycobacterium tuberculosis-reactive CD8+ T lymphocytes: the relative contribution of classical versus nonclassical HLA restriction.* J Immunol, 2000. **165**(2): p. 925-30.
51. Harriff, M.J., et al., *Human Lung Epithelial Cells Contain Mycobacterium tuberculosis in a Late Endosomal Vacuole and Are Efficiently Recognized by CD8+ T Cells.* PLOS ONE, 2014. **9**(5): p. e97515.
52. Laugel, B., et al., *Engineering of Isogenic Cells Deficient for MR1 with a CRISPR/Cas9 Lentiviral System: Tools To Study Microbial Antigen Processing and Presentation to Human MR1-Restricted T Cells.* J Immunol, 2016. **197**(3): p. 971-82.
53. Olive, A.J., et al., *Chlamydia trachomatis-induced alterations in the host cell proteome are required for intracellular growth.* Cell Host Microbe, 2014. **15**(1): p. 113-24.
54. Murhammer, D.W.e., *Baculovirus and insect cell expression protocols*. Methods in Molecular Biology. Vol. 388. 2007, Totowa, NJ: Humana Press.
55. Heinzel, A.S., et al., *HLA-E-dependent presentation of Mtb-derived antigen to human CD8+ T cells.* J Exp Med, 2002. **196**(11): p. 1473-81.
56. Li, K., et al., *Synthesis, stabilization, and characterization of the MR1 ligand precursor 5-amino-6-D-ribitylaminouracil (5-A-RU).* PLoS One, 2018. **13**(2): p. e0191837.
57. López-Sagaseta, J., et al., *The molecular basis for Mucosal-Associated Invariant T cell recognition of MR1 proteins.* Proc Natl Acad Sci U S A, 2013. **110**(19): p. E1771-8.
58. Boulter, J.M., et al., *Stable, soluble T-cell receptor molecules for crystallization and therapeutics.* Protein Eng, 2003. **16**(9): p. 707-11.
59. Chang, H.C., et al., *A general method for facilitating heterodimeric pairing between two proteins: application to expression of alpha and beta T-cell receptor extracellular segments.* Proc Natl Acad Sci U S A, 1994. **91**(24): p. 11408-12.
60. Luoma, A.M., et al., *Crystal structure of Vδ1 T cell receptor in complex with CD1d-sulfatide shows MHC-like recognition of a self-lipid by human γδ T cells.* Immunity, 2013. **39**(6): p. 1032-42.
61. Benveniste, P.M., et al., *Generation and molecular recognition of melanoma-associated antigen-specific human γδ T cells.* Sci Immunol, 2018. **3**(30).
62. Chivers, C.E., et al., *A streptavidin variant with slower biotin dissociation and increased mechanostability.* Nat Methods, 2010. **7**(5): p. 391-3.

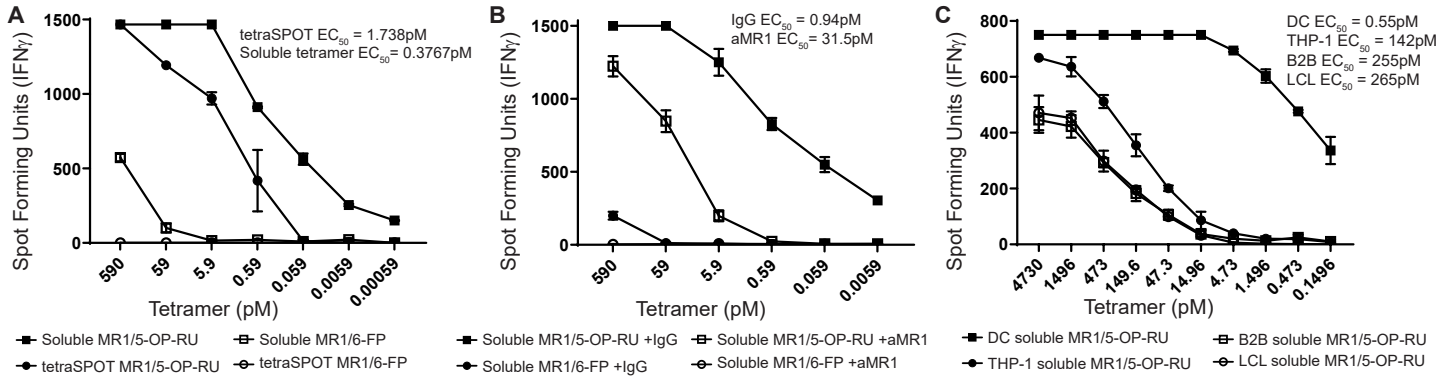

Figure 1

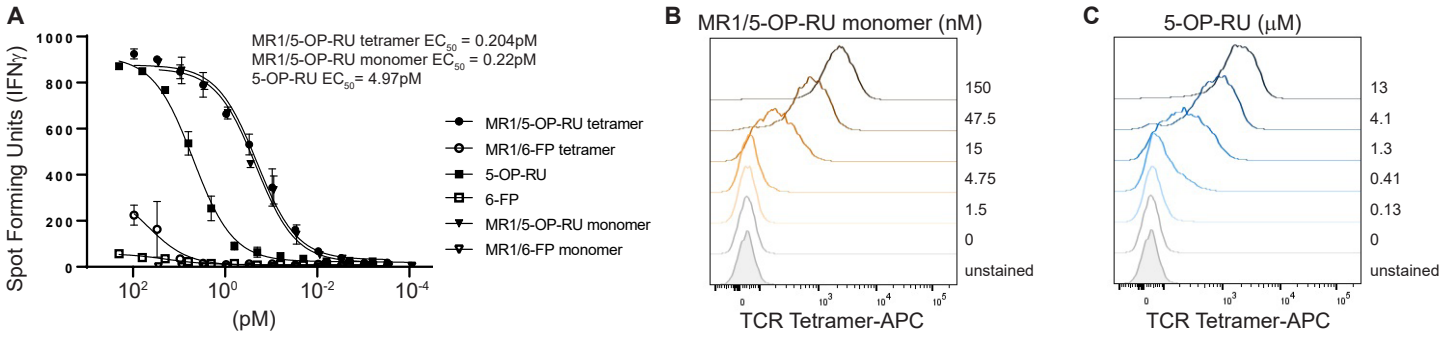

Figure 2

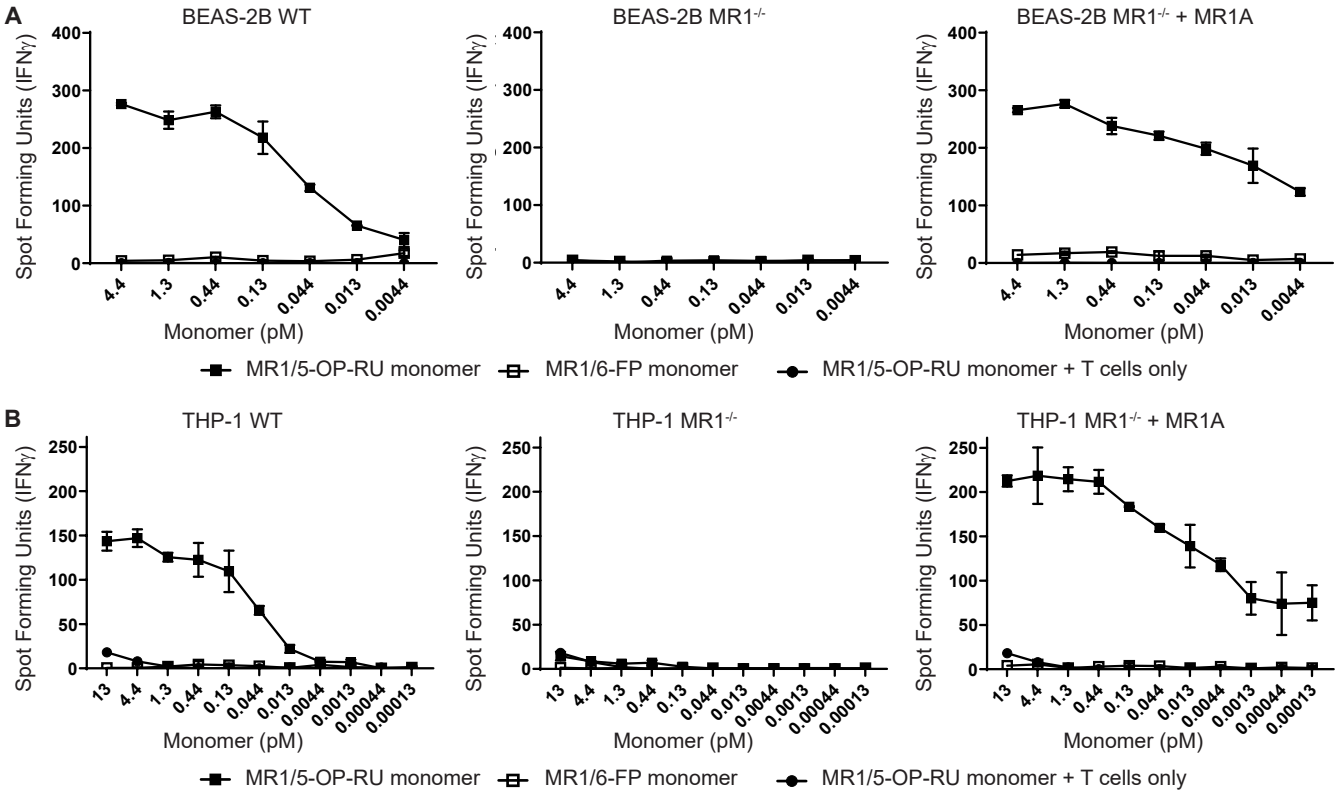

Figure 3

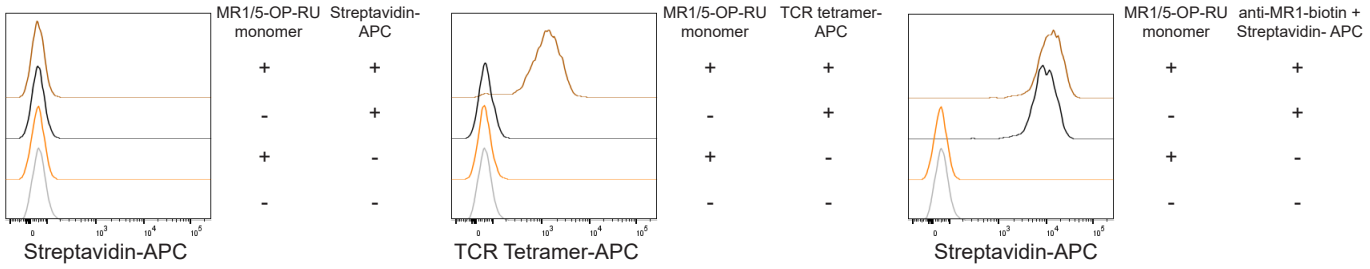

Figure 4

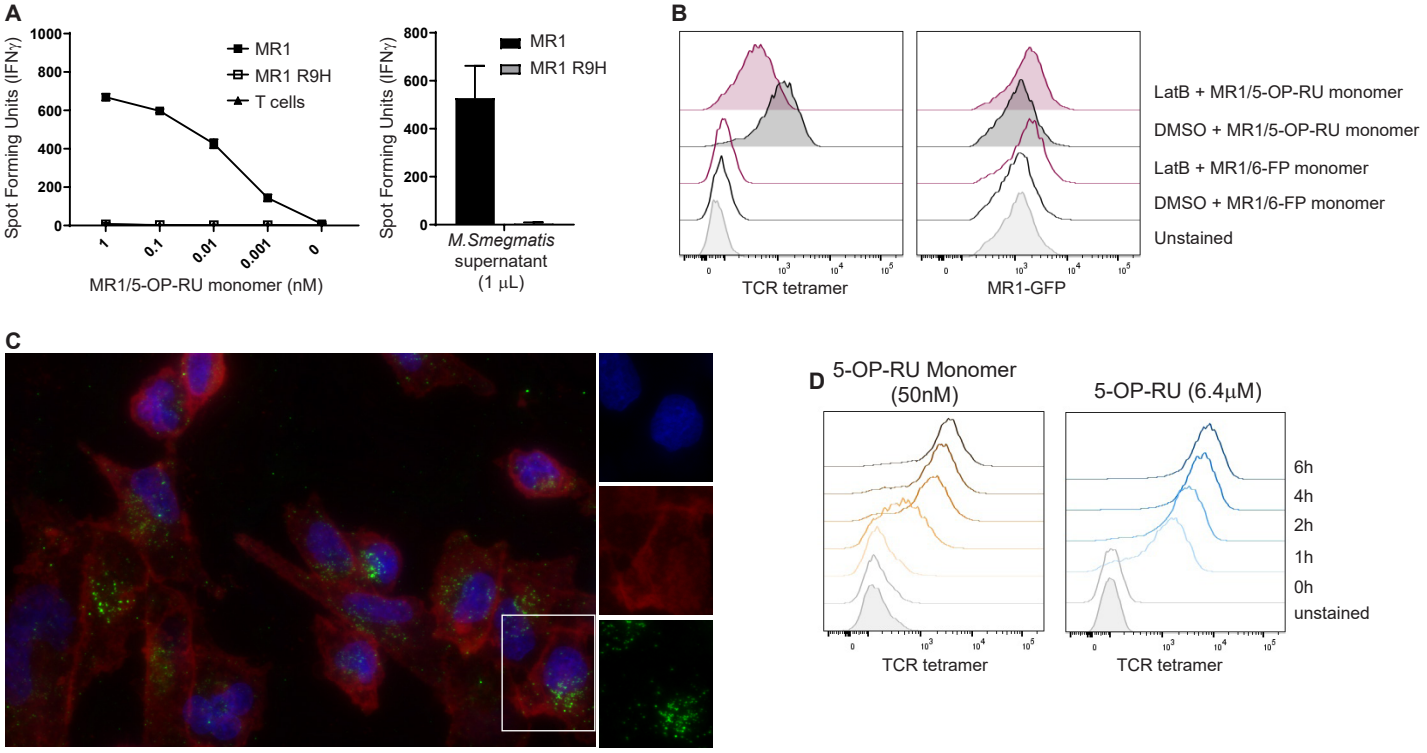

Figure 5

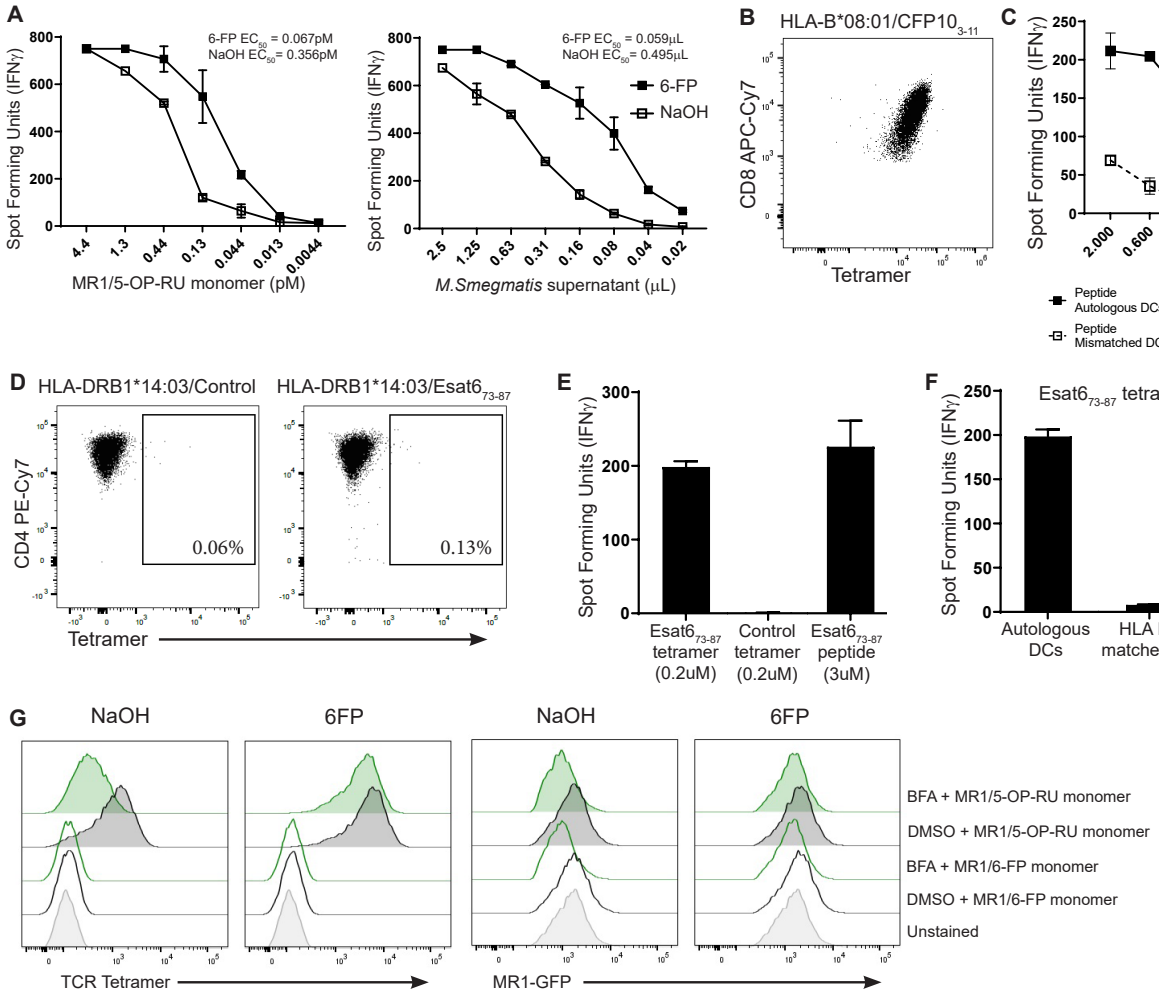

Figure 6

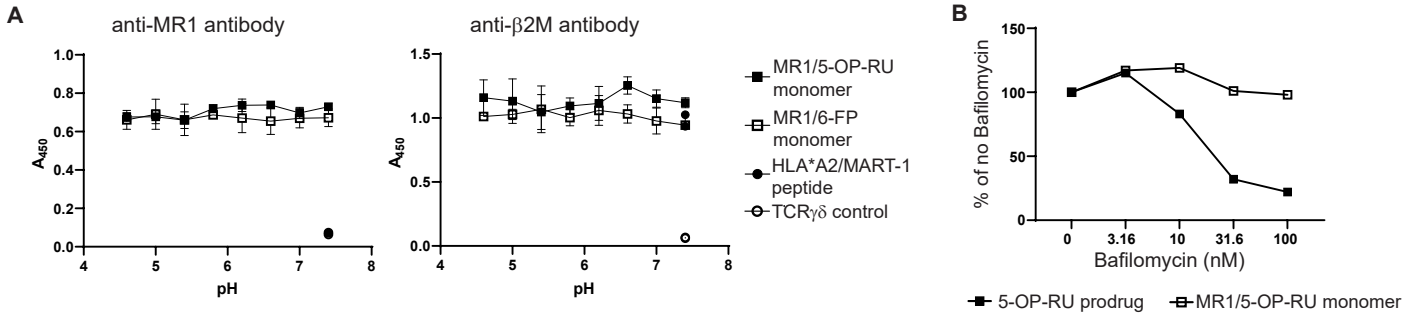

Figure 7